Electroluminescence from Conjugated Polymer Electrospun Nanofibers in Solution Processable Organic Light-Emitting Diodes

Varun Vohra,[†,‡,*] Umberto Giovanella,[†] Riccardo Tubino,[§] Hideyuki Murata,[‡] and Chiara Botta[†]

[†]Istituto per lo Studio delle Macromolecole (ISMac-CNR), Via Bassini, 15, Milan 20133, Italy, [‡]School of Materials Science, Japan Advanced Institute of Science and Technology (JAIST), 1-1 Asahidai, Nomi, Ishikawa 923-1292, Japan, and [§]Universita di Milano-Bicocca/Scienza dei Materiali, Via Roberto Cozzi 53, 20125 Milan, Italy

ABSTRACT Nanofibers of poly[(9,9-dioctylfluorenyl-2,7-diyl)-alt-*co*-(1,4-benzo-{2,1′,3}-thiadiazole)] (F8BT) blended in polystyrene (PS) or polyethylene oxide (PEO) show different diameters and morphology according to the conjugated polymer concentration. Electroluminescence from ribbonlike F8BT nanofibers, obtained by an annealing process of the F8BT/PEO blend, is successfully obtained by applying 6 V bias. Electrical connection is achieved by incorporating the F8BT fibers of about 700 nm width and 110 nm height into a single layer organic light emitting device, whose architecture induces charge recombination on the conjugated polymer nanofibers. This simple method to electrically connect the conjugated polymer nanofibers offers a great potential for low-cost flexible nanodevice fabrication.

KEYWORDS: OLED · nanofibers · conjugated polymer · electroluminescence · electrospinning

The organic light-emitting diode (OLED) technology provides a very attractive and low cost alternative to inorganic materials in fields such as lighting and display applications.[1−3] The peculiar properties of π-conjugated polymers explains why they are considered interesting materials when it comes to the development of low-cost organic electronics technology.[4−6] The challenge is to be able to use them on the nanometer scale in order to fully exploit their flexibility and potential and to combine them with the latest developments in nanoscience.[7−10] Connection of conjugated polymer based nanofibers to electrodes makes the probing of their electrical properties possible and represents an important step toward the realization of a nanoscale OLED.[11] Previous studies have demonstrated the advantages which can result from having elaborated nonplanar architectures such as fiber-shaped OLEDs.[12,13] Moreover, fiber-shaped OLEDs could have a wide range of applications including integration of light sources in fabrics and low cost lighting. The electrospinning process[14−18] can be used to easily obtain such nonplanar architectures at the nanoscale[19] as it provides a low-cost and continuous technique to produce extremely flexible high aspect ratio nanofibers. During the electrospinning of a blend of polymers, phase segregation can occur.[20] Luminescent nanofibers obtained from electrospun blends of polymers have drawn increasing attention in the past few years as they present interesting properties both on the optical and the energy and charge transport point of views.[20−22] Although previous studies have demonstrated electroluminescence from dye-loaded nanofibers,[19] electroluminescence from electrospun conjugated polymer-based nanofibers has never been investigated before.

The way electrical connections from the contacts of the macroscopic device to the active nanosized material are created is crucial in nanodevice technology. In the past years, different ideas to achieve such contacts have been proposed, either by defining the area of the electrical contacts or by confining the size of the active material, and different technologies have been employed, spanning from electron beam lithography to soft nanolithography.[9]

Blending a conjugated polymer with a polymer with good viscoelastic properties, we obtain different dimensions and properties of the electrospun fibers. The study of these fibers allows us to choose the adequate ones to prepare, for the first time, a device based on light-emitting electrospun nanofibers of a conjugated polymer. In the present article, we realize electrical connections to an active polymeric nanofiber using the simple and well developed technology of solution processed OLEDs combined with

* Address correspondence to varunvohra1984@gmail.com.

Received for review March 18, 2011 and accepted June 2, 2011.

Published online June 02, 2011
10.1021/nn201029c

the electrospinning technique. The electrical connection of the nanofiber to the macroscopic device is achieved by embedding them into a planar OLED whose architecture induces the current to specifically flow through the nanofibers. With this simple, easy, and cost-effective route, we verify that electrospun nanofibers based on conjugated polymer can be electrically addressed and yield very efficient electroluminescence therefore opening new perspectives for the fabrication of fiber-shaped nanodevices.

The first part of the study concerns the electrospinning of fibers obtained with a blend of poly[(9,9-dioctylfluorenyl-2,7-diyl)-alt-*co*-(1,4-benzo-{2,1′,3}-thiadiazole)] (F8BT) and a polymer with good viscoelastic properties (used to help the electrospinning process of the rigid unstretchable F8BT backbone). This study allows us to choose the best candidate to build a conjugated polymer nanofiber device. The polymers chosen to be blended with F8BT are polyethylene oxide (PEO) and polystyrene (PS). These two polymers have different polarities and therefore, different affinities with F8BT.

PS is more compatible with F8BT than PEO. Therefore phase segregation is more likely to occur in the fibers based on the F8BT/PEO blends. Blends with different weight ratios of F8BT/PS in toluene were electrospun. With a high concentration of PS (more than 40 wt %), smooth fibers are obtained with a diameter down to around 500 nm. On the other hand, when the concentration of PS is kept under 30 wt %, no fibers are obtained (only droplets are formed during the electrospinning process). In a previous study we showed that F8BT/PS fibers display polarized photoluminescence.[21] This phenomenon is related to the alignment of the polymer chains during the electrospinning process: during the fiber formation, polymer chains are stretched in the direction of the fiber. All the fibers obtained in this work with the different concentrations of PS exhibit the same alignment of the transition dipole moment along the fiber axis. Figure 1 displays fluorescence micrographs obtained with two perpendicular polarized excitations on a single F8BT/PS nanofiber (60 wt % of PS). The fluorescent emission under these conditions clearly shows that the transition dipole moment of the emitting material (F8BT), and therefore the polymer chain axis, is parallel to the nanofiber axis.

Different sets of fibers of F8BT/PEO are obtained from chloroform solutions with PEO concentrations of 15, 25, 35, 50, and 60 wt %. The dimensions of the fibers vary extremely when changing the concentration of PEO. Low PEO concentration fibers have diameters ranging from 700 nm up to a few micrometers whereas the fibers with 35 wt % and over have a rather monodisperse diameter in the range of hundreds of nanometers (typically F8BT/PEO fibers with 35 wt % PEO have a diameter of 500 nm). Unlike the nanofibers

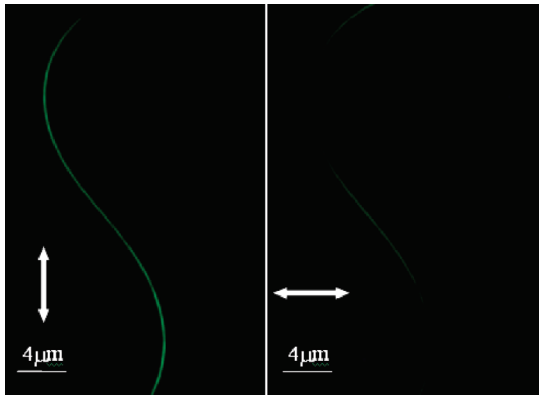

Figure 1. Fluorescence microscope images of nanofibers obtained with 60 wt % of PS excited at 488 nm with a vertically and horizontally polarized light source. The white arrows indicate the direction of the polarization.

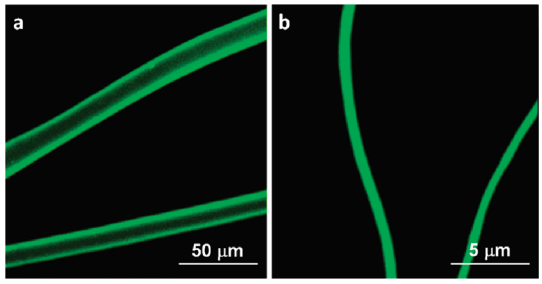

Figure 2. Confocal microscope images of fibers obtained with (a) 15 wt % and (b) 35 wt % of PEO blended with F8BT.

obtained with F8BT/PS blends, the fibers obtained using PEO do not display any polarization of the fluorescence. This is related to the fact that PEO has less affinity with F8BT than PS. The F8BT chains, due to their rigid backbone, have low stretching properties and therefore cannot align on their own. The compatibility between PS and F8BT allows the PS chains to drag the F8BT chains, whereas the low miscibility of PEO and F8BT likely leads to polymer segregation that impedes the alignment of the F8BT chains along the PEO chains.

Figure 2 displays confocal microscope images of fibers obtained with 15 and 35 wt % of PEO. The fibers obtained with 15 wt % of PEO are clearly too large to be used in an OLED type device. A more accurate inspection of the changes in morphology of the nanofibers and the phase segregation which is induced by electrospinning the two polymers will be the subject of a future study.

The main objective of this work is to build a functional device based on nanofibers. We choose a simple device architecture, shown in Figure 3, that allows the fabrication of the devices with low-cost solution-based techniques. Devices with the architecture presented in Figure 3 will possess good performances only if certain required conditions are fulfilled. The thickness of the active layer of the OLED must be quite homogeneous

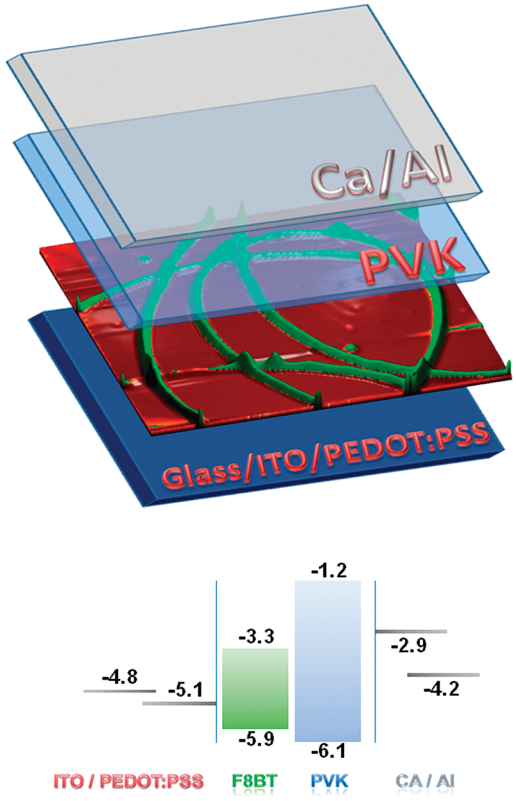

Figure 3. Schematic representation of the OLED structure (top) and energy levels diagram[23,24] (bottom).

in order to avoid dysfunctions and must be kept lower than 200 nm to have enough current flow through the active layer at low voltages. In a layer by layer device, it is also very important that the process used to cover the underlying layer does not dissolve nor destroy it. In our devices, the active layer is made of nanofibers coated with a charge transporting material (typically spin coated from apolar solvents such as toluene). One of the major issues to fabricate those devices concerns the fact that the as-spun nanofibers are soluble in toluene. Taking all these aspects into account, two potential candidates for making such devices are the fibers obtained with F8BT and, respectively, 50 wt % of PS and 35 wt % of PEO. These fibers correspond to the lowest diameters obtained with PS and PEO. The mean height of those two types of fibers is 500 nm which is still too large to have a functional device based on them. The electrospinning process was operated for a short time in order to avoid the fabrication of a mesh of fibers and obtain only single nanofibers separated one from each others. In average, 40% of the surface of the active layer was covered by nanofibers.

Owing to the chemical nature of PS, the fibers based on PS are more soluble into toluene than the ones based on PEO. Furthermore, after annealing at 150 °C, the nanofibers of F8BT/PEO undergo a change in shape and become ribbonlike, while the fibers based on F8BT/PS exhibit no morphological change. The different behaviors of the blends are related to the thermal properties of the polymers. PEO has a melting temperature of 65 °C, whereas the glass transition temperature and the melting temperature of PS are, respectively, 110 and 240 °C. The annealing at 150 °C only gives some mobility to the polymer chains in the F8BT/PS nanofibers as it is above the glass transition temperature of PS but under its melting temperature. The fibers remain 500 nm sized and therefore cannot be used in devices. On the other hand, the PEO present in the F8BT/PEO nanofibers melts, which explains the change of morphology and the crawling of the nanofiber which becomes ribbonlike. To understand better what occurs during the annealing of the F8BT/PEO fibers, a thin spin-coated film of the same blend was prepared and annealed in the same conditions. Fluorescence microscopy and AFM topography images (see Supporting Information, Figure SI1) of the unannealed and annealed films clearly show that there is a remarkable phase separation between the two polymers after the annealing step. F8BT can therefore be considered as poorly soluble in molten PEO.

The AFM images along with the cross sections of the electrospun fibers on glass before and after annealing in Figure 4 show that a change of structure of the nanofibers occurs through the thermal energy given to the polymer chains. Fibers which had a tubular structure with a mean diameter of 500 nm become ribbonlike with a mean height of 110 nm and a mean width of 700 nm. During the annealing step of the F8BT/PEO nanofibers, the PEO separates from the F8BT and flows to the empty spaces between the fibers thus creating a thin layer of wide band gap material covering the surface in between the fibers. Both annealed and unannealed samples were scratched away from the nanofibers in order to observe the PEO layer that is formed and characterize its height (see Supporting Information, Figure SI2). In the unannealed samples, no height difference was measured. In the annealed samples, the height measurements close and across the scratch revealed the formation of a continuous layer between the nanofibers of around 26 nm of thickness. The formation of this PEO layer allows the acquisition of a specific electrical contact of the network of thin nanofibers since the film surrounding the fibers becomes electrically insulating. Furthermore, in a previous study, it has been demonstrated that the thermal annealing at 150 °C of F8BT leads to a partial crystallization of the polymer chains which become less soluble in solvents such as toluene.[25] The annealing step therefore not only induces a significant height reduction of the fibers but also increases their resistance to dissolution in toluene.

Consecutively, the poly(*N*-vinylcarbazole) (PVK) solution is spin-coated on top of the annealed and unannealed fibers and the resulting films are studied in parallel with AFM and fluorescence microscopy

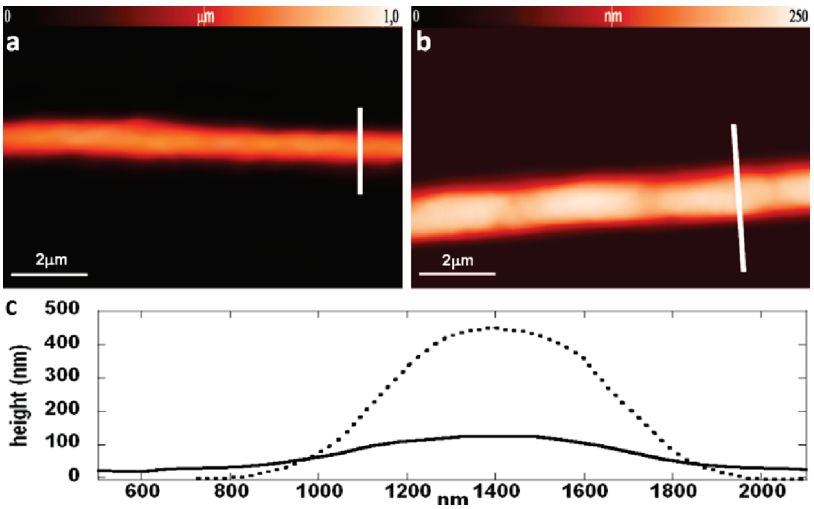

Figure 4. AFM images of nanofibers of F8BT/PEO on glass before (a) and after (b) annealing and their cross sections (c). The cross sections are adjusted by measuring the thickness after scratching the film. Unannealed and annealed fibers' cross sections are respectively represented by the dotted and the solid lines.

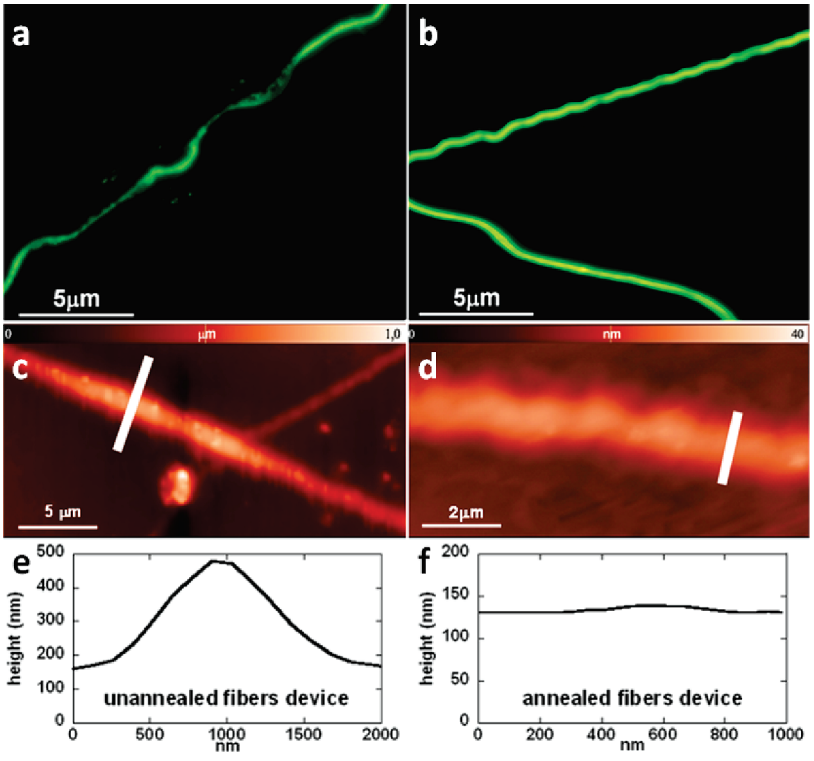

Figure 5. Fluorescence microscopy images (a,b) of fibers of F8BT-PEO on poly(3,4-ethylenedioxythiophene) poly-(styrenesulfonate) (PEDOT:PSS) covered with spin-coated PVK. AFM images (c,d) and cross sections (e,f) of the fibers on glass after the PVK covering step. The height of the PVK film on the cross sections is adjusted by measurements made after scratching the films. The fibers were either left untreated (a,c,e) or annealed at 150 °C for 30 min (b,d,e) before depositing the PVK layer.

(Figure 5). While the untreated nanofibers lose their shape due to partial dissolution in toluene, the annealed nanofibers keep their morphology due to the crystallization of F8BT chains. The thin layer of PEO obtained after annealing the nanofibers is partially dissolved by toluene leading to the formation of a concentration gradient of PEO in the PVK layer formed between the nanofibers (high concentration of PEO close to the substrate). Figure 5 panels a and c show that the partial dissolution of the unannealed nanofibers induces the partial dispersion of F8BT in the PVK film. On the contrary, the ribbonlike structure of the annealed fibers remains entirely undissolved after spin coating the PVK layer (Figure 5b,d). Figures 4 and 5 are

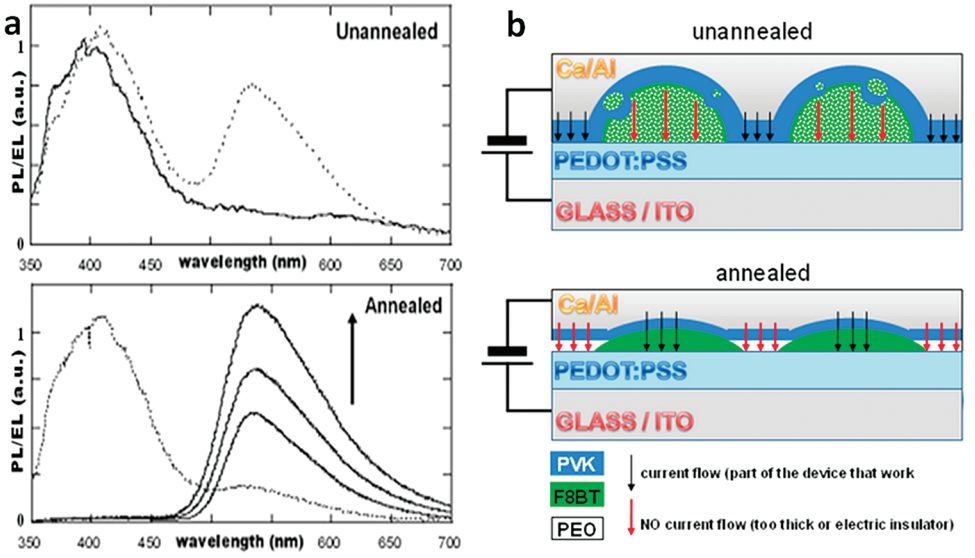

Figure 6. (a) Normalized electroluminescence (solid) and photoluminescence (dotted) spectra of unannealed and annealed fibers of F8BT-PEO in devices. Photoluminescence is obtained by exciting at 300 nm. Electroluminescence is obtained by applying 6 V to the unannealed fibers device and by applying voltages ranging from 6 to 15 V to the annealed fibers device. The arrow shows the increasing voltage. (b) Schematic drawings of the device architectures of the unannealed and annealed fibers devices.

representative of what is typically seen throughout the whole active layer: a careful study of the whole active area of the devices based on annealed fibers with the fluorescence microscope is done to verify that no F8BT is dispersed in the PVK during the covering step. The flattening of the annealed fibers is crucial for the device to work properly since it reduces the thickness and the dishomogeneities of the active layer. The cross sections obtained after PVK is spin coated on the nanofibers (Figure 5e,f) show a surface roughness of around 30 nm for the devices containing annealed fibers, whereas the ones containing untreated fibers display dishomogeneities up to 300 nm.

Annealing the F8BT/PEO nanofibers at 150 °C for 30 min is therefore a crucial step in the device preparation since it allows (i) the creation of a solution processed homogeneous thin active layer of less than 150 nm after PVK spin coating, (ii) the formation of a PEO thin film between the nanofibers, and (iii) the avoidance of the partial dissolution of F8BT and therefore the dispersion of the conjugated polymer into the PVK film. To make the devices, nanofibers are collected on poly(3,4-ethylenedioxythiophene) poly(styrenesulfonate) (PEDOT:PSS) covered ITO substrates and subsequently covered with PVK. To finalize the devices, 30 nm of calcium and 70 nm of aluminum are evaporated on top of the PVK layer and serve as the cathode.

To accurately study these systems, we first investigate the influence of PEO in the devices by preparing devices based on thin spin-coated layers of the F8BT/PEO blend, and we study the influence of the annealing step on the electroluminescence of the blend. No significant changes are observed between the electroluminescence of the unannealed and annealed devices (annealing in the same condition as the fibers; 150 °C for 30 min). We then prepare a device having a 25 nm thick spin-coated layer of PEO covered by a 120 nm thick layer of PVK as the active layer in order to study whether this architecture allows the charges to recombine and have electroluminescence from such an active layer. Such devices are compared with those having only PVK as the active layer. Even at high bias (over 30 V), very low electroluminescence is seen from the devices having the PEO concentration gradient (see Supporting Information, Figure SI3). The insulating PEO layer therefore seems to act as a hole blocking layer which impedes the injection of positive charges into the active layer.[26] Devices prepared with PVK as the active layer with and without the PEO underlying layer have maximum external quantum efficiencies (EQE) of, respectively, 0.5% and less than 0.1%.

Finally, five different sets of devices based on annealed and unannealed nanofibers are fabricated and characterized. The devices made without annealing of the fibers exhibit electroluminescence from the PVK and display very low emission from the F8BT (Figure 6a). The large inhomogeneities in film thickness (around 300 nm) between the regions of the active layer containing the nanofibers and the one containing only PVK induces the current to flow mainly in the thinnest PVK regions of the devices, and therefore a low EQE is measured. The corresponding photoluminescence spectra exhibit emissions from both PVK and F8BT. For this device, since F8BT is partly dispersed in PVK (Figure 5a,c), both the emissions from direct excitation of F8BT and that due to energy transfer from PVK to F8BT are present. Moreover, the strong F8BT emission is related to the high solid-state photoluminescence quantum

yield of F8BT compared to that of PVK, being 0.5 and 0.1, respectively.

On the other hand, as shown in Figure 6a, devices made with annealed fibers display mainly electroluminescence from F8BT, peaked at about 540 nm, with an onset at around 4 V. The emission that we observe in this case comes from the fibers as no F8BT is dispersed in PVK (Figure 5b,d). This is confirmed by the photoluminescence spectra of the device obtained under PVK excitation that displays mainly emission from PVK, with a weaker contribution from F8BT with respect to the unannealed one (Figure 6a). The reduction of the energy transfer from PVK to F8BT, which can be explained by a reduction of the F8BT/PVK interfaces, supports the hypothesis of undissolved fibers. The active layer of these devices is made of 700 nm large and 110 nm thick F8BT nanofibers and a thin layer of PEO that fills the space between fibers, the whole system being covered by spin-coated PVK. Through a simple solution process, the PVK, which cannot be coelectrospun and phase separated from F8BT, allows the formation of a homogeneous active layer with both carrier balancing and radiative exciton blocking properties,[27] while the PEO specifically insulates the area between the fibers giving way to an active layer where fibers can be selectively addressed.

The device areas containing the thin PEO layer, created by the annealing process, are electrically insulating compared to F8BT. Since F8BT acts as an efficient trap for both electrons from PVK and holes directly injected from the anode (see energy levels in Figure 3), electron−hole pairs recombine radiatively into the nanofibers. The bias of the devices can easily be increased to 15 V without seeing almost any emission from PVK. The maximum EQE of 0.7% for the devices based on untreated nanofibers is enhanced to 1.1% upon annealing of the nanofibers, corresponding to the maximum EQE obtained for devices based on active layers of F8BT. The measured luminances for devices based on untreated and annealed nanofibers are, respectively, 36 cd/m^2 at 8.6 V and 2300 cd/m^2 at 6 V. The devices based on unannealed fibers therefore seem to act as PVK-only active layer devices, whereas the annealed nanofibers devices behave like F8BT devices. The model proposed in the scheme in Figure 6b is therefore a very plausible hypothesis.

In conclusion, for the first time electroluminescence from electrospun conjugated polymer nanofibers is obtained. Ribbonlike nanofibers of an electroluminescent polymer (F8BT) are used as active material in OLEDs with a brightness of 2300 cd/m^2 at 6 V. Smooth fibers are produced by electrospinning a blend of F8BT with PEO. PEO is then extracted from the nanofiber in order to obtain a high concentration of F8BT in the nanofiber through a proper annealing step. This annealing step also leads to a flattening and a crystallization of the nanofibers which allow the fabrication of a solution-processable device with a simple planar geometry where the nanofibres are electrically connected. The thin PEO layer created during the annealing step between the nanofibers is electrically inactive and allows selectively addressing the nanofibers. Both electrons and holes are injected in the area of the active layer containing the nanofibers and recombine on the conjugated polymer nanofiber to produce electroluminescence. This simple and novel way of electrically addressing electrospun nanofibers allows full exploitation of the optoelectronic and viscoelastic properties of blends based on conjugated polymers in the field of flexible organic electronics nanotechnology. The nanoworld with its peculiar and interesting properties can therefore be connected with the macroworld of devices which brings us one step closer to fabricating challenging devices such as single nanofiber-based nanodevice for OLED applications.

EXPERIMENTAL SECTION

Preparation of the Nanofibers. The electrospinning apparatus consists of a high voltage power supply (FC 30R04 Glasmman), a 0.5 mm diameter glass capillary containing a platinum-wire electrode and collector-screen counter-electrode placed 20 cm below the capillary tip. The applied potential between the electrodes is 30 kV. The deposition of droplets on the collecting substrate is avoided by using an almost horizontal setup: fibers are collected directly on the substrate, whereas droplets formed during the initiation of the process fall vertically due to gravitational forces. The electrospun solution is a blend of F8BT (American Dye Source Inc., ADS133YE) and PEO (Sigma Aldrich) in chloroform or FBT and PS (Sigma Aldrich) in toluene. Typically, for blends of F8BT/PEO, 30 mg of polymer are added to 1 mL of chloroform and placed in an ultrasonic bath for 10 min at room temperature. For F8BT/PS blends, 100 to 150 mg of polymer are added to 1 mL of toluene. The fibers are collected on glass substrates or PEDOT:PSS covered ITO.

Preparation of the Devices Based on Nanofibers. After treatment with nitrogen plasma, 50 nm of PEDOT:PSS (Clevios P VP AI 4083, H.C. Starck) used as a hole-injection layer at the anode interface is spin-coated onto cleaned ITO substrates, and then dried under nitrogen atmosphere at 100 °C for 10 min. These substrates are placed between the capillary and the counter-electrode to directly collect the nanofibers on the PEDOT:PSS layer.

Once the nanofibers are deposited on the PEDOT:PSS and ITO covered substrate, half of the substrates are placed for annealing on a hot plate at 150 °C under nitrogen flow for 30 min and half of them are kept unannealed in a nitrogen atmosphere. A PVK solution (20 mg/mL) in toluene is then spin-coated on top of the fibers at 2000 rpm for 1 min inside a nitrogen filled drybox. A thin layer of calcium (30 nm) and subsequently a 70 nm layer of aluminum were deposited on the top by vacuum (10^{-7} mbar) thermoevaporation. The active area of the devices is 0.04 cm^2.

Optoelectrical Characterization, Optical and Atomic Force Microscopy. UV−vis transmission spectra were obtained with a Lambda-9

spectrometer. The photoluminescence and electroluminescence spectra were recorded by using a 270 M SPEX spectrometer equipped with a N_2-cooled CCD by exciting with a monochromatized xenon lamp. The spectra were corrected for the instrument response. Fluorescence micrographs were obtained through excitation with a 100 W Hg lamp with a filtered excitation (BA excitation 450−490 nm, observation between 505 and 520 nm). Confocal and fluorescence images were collected with a Nikon Eclipse TE2000-U inverted confocal microscope with a long working distance and using a Plan Fluor objective (magnification 40, N.A. = 0.75). The measurements were done with two excitation wavelengths using a DAPI diode laser at 407 nm and an Ar^+-ion laser at 488 nm.

AFM investigations of the surface topography (height) were performed using the semicontact mode of a NT-MDT NTEGRA apparatus. The thicknesses of the different active layers were obtained by scratching the thin films and measuring the height with the AFM apparatus. Solid-state photoluminescence quantum yields were obtained by using a homemade integrating sphere. Current−voltage (*I*−*V*) characteristics were recorded with a Keithley 2602 source meter. The luminance of the device was measured with a calibrated photodiode. The external quantum efficiency in forward direction (EQE) was derived, by supposing a lambertian source behavior, according to the procedure reported elsewhere.[27]

Acknowledgment. The work was supported by the European Commission through the Human Potential Program (Marie-Curie RTN "Nanomatch" Contract No. MRTN-CT-2006-035884; www.nanomatch.eu) and by a Grant-in-Aid for ScientificResearch on Innovative Areas (No. 20108012, "π-Space") from the Ministry of Education, Culture, Sports, Science, and Technology, Japan.

Supporting Information Available: (SI1) Fluorescence and AFM microscopy images of the phase segregation upon annealing of the blend of F8BT/PEO. (SI2) AFM profile of the thin PEO film formed between two adjacent nanofibers. (SI3) Current−voltage and brightness−voltage curves of the devices based on PVK with and without the underlying thin PEO layer. (SI4) Current−voltage and brightness−voltage curves of the untreated and annealed nanofibers devices. This material is available free of charge *via* the Internet at http://pubs.acs.org.

REFERENCES AND NOTES

1. Müllen, K. Scherf, U. *Organic Light Emitting Devices: Synthesis, Properties and Applications*; Wiley-VCH, Inc: Germany, 2006.
2. Burroughes, J. H.; Bradley, D. D. C.; Brown, A. R.; Marks, R. N.; Mackay, K.; Friend, R. H.; Burn, P. L.; Holmes, A. B. Light-Emitting Diodes Based on Conjugated Polymers. *Nature* **1990**, *347*, 539–541.
3. Lee, P.-I.; Hsu, S. L.-C.; Lee, R.-F. White-Light-Emitting Diodes from Single Polymer Systems Based on Polyfluorene Copolymers End-Capped with a Dye. *Polymer* **2007**, *48*, 110–115.
4. Hines, D. R.; Southard, A.; Fuhrer, S. Poly(3-hexylthiophene) Thin-Film Transistors with Variable Polymer Dielectrics for Transfer-Printed Flexible Electronics. *J. Appl. Phys.* **2008**, *104*, 024510.
5. Bolognesi, A.; Botta, C.; Facchinetti, D.; Jandke, M.; Kreger, K.; Strohriegl, P.; Relini, A.; Rolandi, R.; Blumstengel., S. Polarized Electroluminescence in Double-Layer Light-Emitting Diodes with Perpendicularly Oriented Polymers. *Adv. Mater.* **2001**, *13*, 1072–1075.
6. Millefiorini, S.; Kozma, E.; Catellani, M.; Luzzati, S. Dithienothiophene Based Polymer as Electron Donor in Plastic Solar Cells. *Thin Solid Films* **2008**, *516*, 7205–7208.
7. Li, H.; Luo, Y.; Shuai, Z.; Kashimura, Y.; Liu, Y.; Torimitsu, K. Advancing Conjugated Polymers into Nanometer-Scale Devices. *Pure Appl. Chem.* **2006**, *78*, 1803–1822.
8. Yamamoto, H.; Wilkinson, J.; Long, J. P.; Busman, K.; Christodoulides, J. A.; Kafafi, Z. H. Nanoscale Conjugated-Polymer Light-Emitting Diodes. *Nano Lett.* **2005**, *5*, 2485–2488.
9. Price, S. P.; Henzie, J.; Odom, T. W. Addressable, Large-Area Nanoscale Organic Light Emitting Diodes. *Small* **2007**, *3*, 372–374.
10. Kim, F. S.; Ren, G.; Jenekhe, S. A. One-Dimensional Nanostructures of π-Conjugated Molecular Systems: Assembly, Properties, and Applications from Photovoltaics, Sensors, and Nanophotonics to Nanoelectronics. *Chem. Mater.* **2011**, *23*, 682–732.
11. Babel, A.; Li, D.; Xia, Y.; Jenekhe, S. A. Electrospun Nanofibers of Blends of Conjugated Polymers: Morphology, Optical Properties, and Field-Effect Transistors. *Macromolecules* **2005**, *38*, 4705–4711.
12. O'Connor, B.; An, K. H.; Zhao, Y.; Pipe, K. P.; Shtein, M. Fiber-Shaped Light Emitting Device. *Adv. Mater.* **2007**, *19*, 3897–3900.
13. Niu, Q.; Zhou, Y.; Wang, L.; Peng, J.; Wang, J.; Pei, J.; Cao, Y. Enhancing the Performance of Polymer Light-Emitting Diodes by Integrating Self-Assembled Organic Nanowires. *Adv. Mater.* **2008**, *20*, 964–969.
14. Huang, Z.-M.; Zhang, Y.-Z.; Kotaki, M.; Ramakrishna, S. A Review on Polymer Nanofibers by Electrospinning and Their Applications in Nanocomposites. *Compos. Sci. Technol.* **2003**, *63*, 2223–2253.
15. Sun, Z.; Zussman, E.; Yarin, A. L.; Wendorff, J. H.; Greiner, A. Compound Core−Shell Polymer Nanofibers by Co-electrospinning. *Adv. Mater.* **2003**, *15*, 1929–1932.
16. Yu, J. H.; Fridrikh, A. V.; Rutledge, G. Production of Submicrometer Diameter Fibers by Two-Fluid Electrospinning. *Adv. Mater.* **2004**, *16*, 1562–1566.
17. Li, D.; Xia, Y. Electrospinning of Nanofibers: Reinventing the Wheel? *Adv. Mater.* **2004**, *16*, 1151–1170.
18. Stanger, J.; Tucker, N.; Kirwan, K.; Staiger, M. P. Effect of Charge Density on the Taylor Cone−Experimental Study. *Int. J. Mod. Phys. B* **2009**, *23*, 1956–1961.
19. Moran-Mirabal, J. M.; Slinker, J. D.; DeFranco, J. A.; Verbridge, S. S.; Ilic, R.; Flores-Torres, S.; Abruna, H.; Malliaras, G. G.; Craighead, H. G. Electrospun Light-Emitting Nanofibers. *Nano Lett.* **2007**, *7*, 458–463.
20. Bianco, A.; Bertarelli, C.; Frisk, S.; Rabolt, J. F.; Gallazzi, M. C.; Zerbi, G. Electrospun Polyalkylthiophene/Polyethyleneoxide Fibers: Optical Characterization. *Synth. Met.* **2007**, *157*, 276–281.
21. Vohra, V.; Devaux, A.; Dieu, L.-Q.; Scavia, G.; Catellani, M.; Calzaferri, G.; Botta, C. Energy Transfer in Fluorescent Nanofibers Embedding Dye-Loaded Zeolite L Crystals. *Adv. Mater.* **2009**, *21*, 1146–1150.
22. Vohra, V.; Calzaferri, G.; Destri, S.; Pasini, M.; Porzio, W.; Botta, C. Toward White Light Emission through Efficient Two-Step Energy Transfer in Hybrid Nanofibers. *ACS Nano* **2010**, *4*, 1409–1416.
23. Morii, K.; Omoto, M.; Ishida, M.; Graetzel, M. Enhanced Hole Injection in a Hybrid Organic−Inorganic Light-Emitting Diode. *Jpn. J. Appl. Phys.* **2008**, *47*, 7366–7368.
24. Parker, I. D.; Pei, Q.; Marrocco, M. Efficient Blue Electroluminescence from a Fluorinated Polyquinoline. *Appl. Phys. Lett.* **1994**, *65*, 1272–1274.
25. Donley, C. L.; Zaumseil, J.; Andreasen, J. W.; Nielsen, M. M.; Stirringhaus, H.; Friend, R. H.; Kim, J.-S. Effects of Packing Structure on the Optoelectronic and Charge Transport Properties in Poly(9,9-di-*n*-octylfluorene-alt-benzothiadiazole). *J. Am. Chem. Soc.* **2005**, *127*, 12890–12899.
26. Park, J. H.; Park, O. O.; Yu, J.-W.; Kim, J. K.; Kim, Y. C. Effect of Polymer-Insulating Nanolayers on Electron Injection in Polymer Light-Emitting Diodes. *Appl. Phys. Lett.* **2004**, *84*, 1783.
27. Giovanella, U.; Betti, P.; Botta, C.; Destri, S.; Moreau, J.; Pasini, M.; Porzio, W.; Vercelli, B.; Bolognesi, A. All-Conjugated Diblock Copolymer Approach To Improve Single Layer Green Electroluminescent Devices. *Chem. Mater.* **2011**, *23*, 810–816.